PCCP

PAPER

View Article Online
View Journal

Cite this: DOI: 10.1039/c8cp01539b

Electron-withdrawing effects on the molecular structure of 2- and 3-nitrobenzonitrile revealed by broadband rotational spectroscopy and their comparison with 4-nitrobenzonitrile†

Jack B. Graneek,[abc] William C. Bailey[d] and Melanie Schnell *[abc]

Received 8th March 2018,
Accepted 31st July 2018

DOI: 10.1039/c8cp01539b

rsc.li/pccp

The rotational spectra of 2- and 3-nitrobenzonitrile were recorded *via* chirped-pulse Fourier transform microwave spectroscopy in the frequency range of 2–8 GHz. These molecules each display large dipole moments, making them viable candidates for deceleration and trapping experiments with AC-electric fields. For both molecules, the main isotopologues and all isotopologues of the respective ^{13}C-, ^{15}N-, ^{18}O-monosubstituted species in their natural abundance were assigned. These assignments allowed for the structural determination of 2- and 3-nitrobenzonitrile *via* Kraitchman's equations as well as a mass-dependent least-squares fitting approach. The experimentally determined structural parameters are then compared to those obtained from quantum-chemical calculations for these two molecules and 4-nitrobenzonitrile. Structural changes caused by steric interaction and competition for the electron density of the phenyl ring highlight how these strong electron-withdrawing substituents affect one another according to their respective positions on the phenyl ring.

1 Introduction

Nitrobenzonitrile (NBN) consists of two electron-withdrawing groups, both of which have negative inductive and mesomeric effects on the phenyl ring. This leads to an electron poor aromatic ring relative to benzene, which can also be described as deactivated. The position of the nitro group with respect to the nitrile group produces three different molecular dipole moments varying in magnitude. The *para* position, corresponding to 4-NBN, produces the weakest molecular dipole moment as it has two electron-withdrawing groups pulling from opposite ends of the phenyl ring. Moving to the *meta* (3-NBN) and *ortho* (2-NBN) positions partly redistributes the electron density of the phenyl ring to one side, resulting in a more polar molecule. As benzonitrile and some of their derivatives display interesting biochemical and physical properties,[1–3] all three NBN molecules have been previously investigated *via* Hartree–Fock and density functional theory methods.[4] Besides the intriguing chemistry that arises from the strongly electron-withdrawing groups present in NBN, part of our motivation stems from the potential application of deceleration and trapping techniques. The large dipole moment to mass ratios for 2-NBN (6.97 D : 148.12 u), and 3-NBN (4.38 D : 148.12 u), together with the ease at which they can be seeded into a molecular beam, make these molecules ideal candidates for experiments that aim to control and manipulate a molecule's motion using external electric,[5] magnetic[6] or electromagnetic fields.[7–9] A detailed knowledge of a molecule's rotational energy level structure, provided by the study of its microwave spectrum, is particularly useful for manipulation experiments that aim to utilise the DC- or AC-Stark effect.[10]

Owing to their polarity, these molecules can be studied using high resolution chirp-pulse Fourier transform microwave (CP-FTMW) spectroscopy. The high sensitivity and resolution offered by this technique allows for the detection of rotational signatures for heavy atom isotopologues, relevant for the determination of structural parameters,[11–14] as well as information on the nuclear quadrupole coupling that arises due to the presence of ^{14}N nuclei in NBN. These, in turn, can provide valuable information on the electronic environment and thus the effect on bonding with the respective nucleus. As of yet,

[a] Deutsches Elektronen-Synchrotron, Notkestraße 85, D-22607 Hamburg, Germany
[b] CAU Kiel, Institute of Physical Chemistry, Max-Eyth-Straße 1, D-24118 Kiel, Germany. E-mail: melanie.schnell@desy.de
[c] Max-Planck-Institut für Struktur und Dynamik der Materie Luruper Chaussee 149, D-22761 Hamburg, Germany
[d] Chemistry-Physics Department, Kean University, 1000 Morris Avenue, Union, NJ, USA

† Electronic supplementary information (ESI) available: Rotational spectroscopy parameters determined *via* a B3LYP/aug-cc-pVTZ (GD3BJ) calculation for each NBN molecule, the calculated NQCCs obtained using the models described in Section 3, the rotational constants determined for each isotopologue of 2- and 3-NBN, experimentally determined and calculated bond lengths/angles of 2- and 3-NBN, as well as the calculated bond lengths/angles of 4-NBN. Lists of all the fitted transitions for each isotopologue of 2- and 3-NBN are also provided. See DOI: 10.1039/c8cp01539b

microwave spectroscopy has not been applied to either 2- or 3-NBN. The almost negligible dipole moment of 4-NBN (0.09 D) makes the acquisition of its pure rotational spectrum difficult. Consequently, we utilize the 4-NBN structures determined *via* quantum-chemical calculations and X-ray crystallography[15] to compare with the structural parameters of 2- and 3-NBN determined in this investigation. Such a comparison provides insight into how the arrangement of the electron-withdrawing substituents on the phenyl ring impacts upon the molecular structures of NBN.

2 Experimental details

The broadband rotational spectra of 2- and 3-NBN were recorded using the Hamburg CP-FTMW COMPACT spectrometer, a detailed description of the set-up can be found in ref. 16. For details concerning recent improvements to the Hamburg spectrometer, such as the incorporation of the 'fast frame' approach,[11] refer to ref. 13. CP-FTMW spectroscopy is a fast, robust and sensitive coherence spectroscopy technique.[17] A broadband microwave chirp is created using an arbitrary waveform generator (AWG), which is coupled into the vacuum chamber. The microwave excitation chirp is amplified by an adjustable travelling wave tube (TWT) amplifier at 50% gain with an output power of approximately 75 W.[14] Due to the large dipole moments of both molecules a 50% gain is preferred over full gain at 100%, which corresponds to an output power between 300–600 W, reasons for this will be discussed later in Section 4. Horn antennas broadcast the microwave chirp into the vacuum chamber where it interacts with a sample of supersonically expanded, internally cold molecules. Polarization of the sample is achieved, and a macroscopic dipole moment is formed when the molecules are resonant with a frequency within the chirp. The decay of this macroscopic dipole moment is recorded as a free induction decay (FID) in the time domain with a high-speed digital oscilloscope.

Phase stability allows for averaging high numbers of acquisitions in the time domain to obtain a good signal to noise (S : N) ratio. For both measurements, a carrier gas of neon was used at a backing pressure of 2.5 bar. Each sample was supersonically expanded into the spectrometer *via* a pulsed nozzle at a repetition rate of 9 Hz. In the case of 2-NBN, approximately 5 million acquisitions were recorded over approximately 19 hours, and after Fourier transformation a rotational spectrum with a S : N ratio of 4000 : 1 was produced. For 3-NBN, approximately 3.1 million acquisitions were recorded over approximately 12 hours, and after Fourier transformation a similar S : N ratio was produced. The S : N ratios of both spectra were fully sufficient to observe the singly substituted ^{13}C-, ^{15}N-, and ^{18}O-isotopologues in their natural abundances of 1.1%, 0.36%, and 0.2%, respectively.

3 Computational details

Quantum-chemical calculations were performed in Gaussian09[18] for all three NBN molecules. Structure optimization calculations were carried out using the aug-cc-pVTZ basis set with the B3LYP hybrid functional including and excluding Grimme's empirical dispersion (GD3BJ). Including Grimme's empirical dispersion resulted in only minor differences to the parameters obtained when it was excluded, thus the later discussion relies on the information obtained *via* the B3LYP/aug-cc-pVTZ calculations for comparison purposes. The obtained rotational parameters, including the nuclear quadrupole coupling constants (NQCCs), of each NBN molecule are listed in Table 1. For the rotational parameters obtained when including Grimme's empirical dispersion refer to Table S1 in the ESI.†

Additional calculations of the NQCCs were also carried out as follows. Molecular structures for 2-, 3- and 4-NBN were obtained by optimization at the B3P86/6-31G(3d,3p) level of theory. On these structures, calculation of the nitrile nitrogen electric field gradients (EFGs) was made with the B3PW91/6-311+G(df,pd) model,[19,20] and converted to NQCCs *via* the factor 4.5586(40) MHz per a.u. For the nitrogen of the nitro group the B3PW91/6-311+G(d,p) model[20,21] was employed, and converted *via* 4.599(12) MHz per a.u. This latter model has proven to be more accurate than the former for pi-electron conjugated nitrogen environments. Otherwise, the former is the

Table 1 Spectroscopic constants of 2-, 3-, 4-nitrobenzonitrile (NBN) determined experimentally and *via* quantum-chemical calculations. N_{11} refers to the nitrogen atom of the nitro group and N_{15} to the nitrogen atom of the nitrile group. For a detailed labelling of the atoms refer to Fig. 2(b), (d) and (e). The standard errors of the obtained values are included in parentheses, and values for the number of lines assigned (N_{lines}) and the root-mean-square deviation of the fit (σ) are also provided

	Experiment		B3LYP/aug-cc-pVTZ		
Parameter	2-NBN	3-NBN	2-NBN	3-NBN	4-NBN
A [MHz]	1506.5484(2)	2269.92862(9)	1499.04	2282.75	3985.67
B [MHz]	1240.8070(6)	749.97847(4)	1254.69	751.43	593.84
C [MHz]	685.2525(5)	563.99011(3)	683.01	565.33	516.84
D_K [kHz]	0.149(5)	—	—	—	—
D_{JK} [kHz]	−0.267(6)	—	—	—	—
D_J [kHz]	0.162(6)	—	—	—	—
χ_{aa} (N_{11}) [MHz]	−0.779(1)	−0.727(2)	−0.9335	−0.8777	−1.1533
$\chi_{bb} - \chi_{cc}$ (N_{11}) [MHz]	−0.470(3)	−0.766(3)	−1.0777	−1.2983	−1.0238
χ_{aa} (N_{15}) [MHz]	−0.401(1)	−2.518(1)	−0.2163	−2.8007	−4.8451
$\chi_{bb} - \chi_{cc}$ (N_{15}) [MHz]	−4.197(2)	−1.528(2)	−5.2325	−1.7141	0.1309
$\mu_a/\mu_b/\mu_c$ [D]	—	—	6.69/1.94/0	0.14/4.38/0	0.09/0/0
N_{lines}	289	256	—	—	—
σ [kHz]	4.9	3.2	—	—	—

Table 2 Comparison of the NQCCs determined experimentally to those obtained *via* the quantum-chemical calculations described in Section 3

	2-NBN			3-NBN		
Parameter	Exp.	B3LYP	B3PW91	Exp.	B3LYP	B3PW91
χ_{aa} (N_{11}) [MHz]	−0.779(1)	−0.9335	−0.805	−0.727(2)	−0.8777	−0.743
$\chi_{bb} - \chi_{cc}$ (N_{11}) [MHz]	−0.470(3)	−1.0777	−0.525	−0.766(3)	−1.2983	−0.749
χ_{ab} (N_{11}) [MHz]	—	−0.2907	−0.357	—	−0.4956	−0.553
χ_{aa} (N_{15}) [MHz]	−0.401(1)	−0.2163	−0.367	−2.518(1)	−2.8007	−2.548
$\chi_{bb} - \chi_{cc}$ (N_{15}) [MHz]	−4.197(2)	−5.2325	−4.607	−1.528(2)	−1.7141	−1.528
χ_{ab} (N_{15}) [MHz]	—	3.2362	2.957		3.2931	2.957

recommended model. These calculated NQCCs are compared with experimentally determined constants in Table 2. Calculated NQCCs of 4-NBN are displayed in the ESI† in Table S2.

4 Results and discussion

The broadband rotational spectra of 2- and 3-NBN measured with the TWT amplifier at 50% gain and the corresponding fits to the asymmetric-rotor Hamiltonian operators are displayed in Fig. 1(a) and (c), respectively. After assignment of the strong a- and b-type transitions for 2- and 3-NBN, respectively, the quantum-chemical rotational parameters could be directly compared to those determined experimentally. The microwave spectrum was fitted using an asymmetric rotor Hamiltonian (Watson S-reduction in the III^l and I^r representations for 2-NBN and 3-NBN, respectively) with the program PGOPHER.[22] It is important to note that for comparison purposes later the quantum-chemical calculations employed do not consider zero-point vibration. The rotational quantum numbers involved in the assigned transitions range from $J = 1$ up to $J = 9$ for 2-NBN, and from $J = 1$ up to $J = 10$ for 3-NBN. In total 289 lines were assigned for the main isotopologue, the parent molecule, of 2-NBN with an average error of the fit of 4.9 kHz. For the parent molecule of 3-NBN, 256 lines were assigned with an average error of the fit of 3.2 kHz.

A 50% gain of the TWT amplifier (corresponding to an output power of approximately 75 W) is utilized in this study to prevent population transfer/inversion and stepwise multi-resonance effects, which have been previously observed for other molecules with large dipole moments and high excitation powers.[14,16] A lower gain can prevent these population-altering effects and lead to a better agreement of transition intensities with those predicted by PGOPHER, thus simplifying the assignment. The rotational temperature of the simulated spectra was set to 1 K, which is the approximate temperature of a supersonically expanded sample of NBN seeded with neon in the experimental set-up. The recorded spectra differ noticeably for each NBN molecule. 2-NBN, a near-oblate molecule with a large μ_a, produces a clear a-type spectrum (Fig. 1(a)), whereas 3-NBN, a near-prolate molecule with a large μ_b, produces a more congested b-type spectrum that is harder to recognize (Fig. 1(c)). For 2-NBN, the measured transition intensities agree reasonably well with those predicted, which is not the case for 3-NBN. The measured transition intensities between 5 and 8 GHz for 3-NBN are clearly weaker than those predicted with PGOPHER. This cannot be a temperature effect, as adjusting the temperature within the range of what is normal for a supersonically expanded sample seeded in neon (1–2 K) offers no improvement to the agreement of transition intensities of 3-NBN. As 3-NBN has a smaller dipole moment (4.38 D) compared to 2-NBN (6.97 D), a larger gain might have been more appropriate. Irrespective of the mismatch in transition intensities a large number of transitions within the 5–8 GHz frequency range could be reliably assigned, because of the high frequency resolution offered by CP-FTMW spectroscopy.

A closer look at the hyperfine structure of 2-NBN due to the nitrogen nuclei of the nitro and nitrile groups can be found in Fig. 1(b). Note for the spectra that display hyperfine structure (Fig. 1(b) and (d)) both the red and blue lines represent the simulated spectra, and only the lines in blue were assigned. The observed hyperfine structure in Fig. 1(b) and (d) arises from the coupling of the two nitrogen atom's nuclear charge density with the electric potential generated by the electrons and other nuclei present in the molecule. For two nuclei that have the same, or comparable, coupling strength the most convenient scheme to describe this coupling interaction is the ($I_1I_2I_{12}JFM_F$) representation.[23] In this scheme the combined nuclear spins (I) of the nitrogen nuclei ($I_1 + I_2 = I_{12}$) couple with the molecular rotational angular momentum J to give a total angular momentum of F, and the new angular momentum quantum numbers are

$$I_{12} = I_1 + I_2,$$

$$F = J + I_{12}$$

Fig. 1(b) and (d) use this coupling scheme to label the quantum numbers involved in the observed transitions.

The NQCCs are not only sensitive to the local electronic environment of the nucleus, but also to the orientation of the principal axis system of the molecule. Fig. 2(a), (c) and (e) show the orientation of the principal axis system for 2-, 3-, and 4-NBN, respectively. Initial calculations mostly predicted more negative values for the NQCCs compared to those determined experimentally. The exception being the experimental χ_{aa} value of the N_{15} atom for 2-NBN, which is almost 200 kHz more negative than the predicted value (refer to Table 1). Further calculations and the application of models described in more detail in ref. 19–21 resulted in a much better agreement of the predicted NQCCs with those determined experimentally (Table 2). For the atom labelling of 2-, 3-, and 4-NBN refer to Fig. 2(b), (d) and (e), respectively. Note that N_{11} and N_{15} consistently refer to the nitrogen atoms of the respective nitro and nitrile groups.

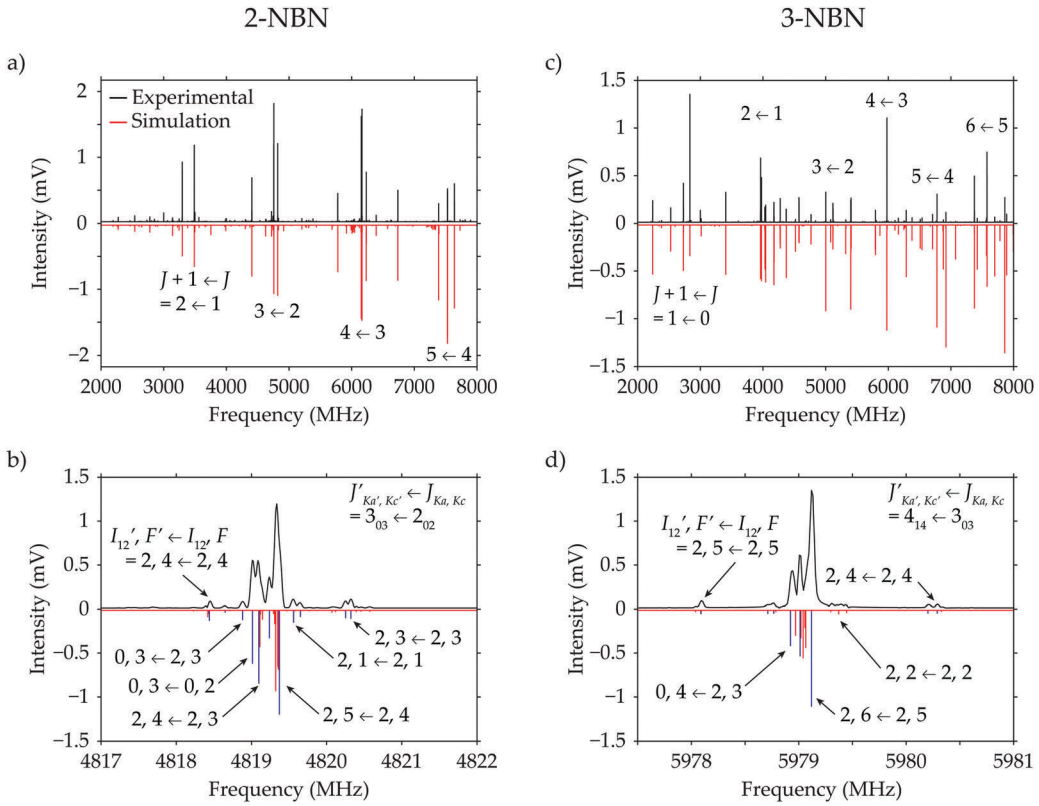

Fig. 1 Broadband rotational spectra of (a) 2-NBN and (c) 3-NBN. Nuclear quadrupole coupling splitting due to the N_{11} (nitro) and N_{15} (nitrile) atoms of (b) 2-NBN and (d) 3-NBN. The F and I_{12} quantum numbers for the $J'_{Ka',Kc'} \leftarrow J_{Ka,Kc} = 3_{03} \leftarrow 2_{02}$ (b) and $4_{14} \leftarrow 3_{03}$ (d) transitions are also displayed. For each plot the lower trace (red/blue) represents a simulation of the fitted spectroscopic parameters reported in Table 1 and has been given an offset for better visibility of the S : N ratio of the experimental spectrum (black). Blue lines included in plots (b) and (d) indicate which lines were assigned, due to the high line density the red lines of these plots were not assigned.

Focusing on the experimental NQCCs and comparing those determined for 2-NBN with 3-NBN, the differences observed for the N_{11} atom relative to the N_{15} atom are much less significant. Changes to the molecular arrangement of NBN causes the principal axis system to reposition accordingly (Fig. 2(a, c and e)). For both 2- and 3-NBN, the N_{11} atom lies close to the *a* inertial axis and is positioned a similar distance away from the centre of mass. The N_{15} atom of 2-NBN lies close to the *b* inertial axis, whereas for 3-NBN, the N_{15} atom is now positioned further away from the centre of mass and closer to the *a*-axis. This repositioning results in comparable NQCCs of the N_{11} atom, but more significant differences for the N_{15} atom (refer to Table 2 and Tables S2 and S3 of the ESI†). Changes to the structure of these molecules will also have an effect on the local electronic environment of the nitrogen nuclei and thus their respective NQCCs. Evaluation of the structural parameters of each molecule should provide more insight into how the local electronic environments of the substituents change according to their position on the phenyl ring.

The high sensitivity of CP-FTMW spectroscopy facilitates the observation of singly substituted ^{13}C-, ^{15}N-, and ^{18}O-isotopologues in their natural abundance for both 2- and 3-NBN. For 2-NBN the lines attributed to the isotopologues of the $J'_{Ka',Kc'} \leftarrow J_{Ka,Kc} = 5_{15} \leftarrow 4_{14}$ and the $5_{05} \leftarrow 4_{04}$ transitions are displayed in Fig. 3(a). Lines for the isotopologues of the $1_{11} \leftarrow 0_{00}$ transition for 3-NBN are displayed in Fig. 3(b). The number of lines assigned and the rotational constants derived from the fits of each isotopologue for 2- and 3-NBN are summarized in the ESI† in Tables S4 and S5, respectively. With this information, both the substituted (r_s) and mass-dependent ($r_m^{(1)}$) coordinates for each of the listed atoms could be determined and compared with the equilibrium (r_e) coordinates obtained *via* quantum-chemical calculations and with each other. The r_e-structure corresponds to a hypothetical equilibrium structure at a potential energy minimum without zero-point vibration.

The r_s-coordinates for 2-NBN were calculated with the KRA program[24] using Kraitchman's equations.[25] For a molecule that displays a large inertial defect ($\Delta = I_c - I_a - I_b$), it is normal protocol to employ the non-planar approach when applying Kraitchman's equations. Inertial defects are usually a result of out-of-plane hydrogens or low-lying out-of-plane vibrations, or even a combination of both.[26,27] Although 2-NBN has an inertial defect of -5.24 μÅ^2 the majority of the r_s-coordinates generated with the non-planar approach produce imaginary components. For this reason, only the r_s-structure determined *via* the planar approach is reported here (refer to Tables S6 and S7 in the ESI†). It has been previously reported that the position of an atom with respect to the molecule's centre of mass or the

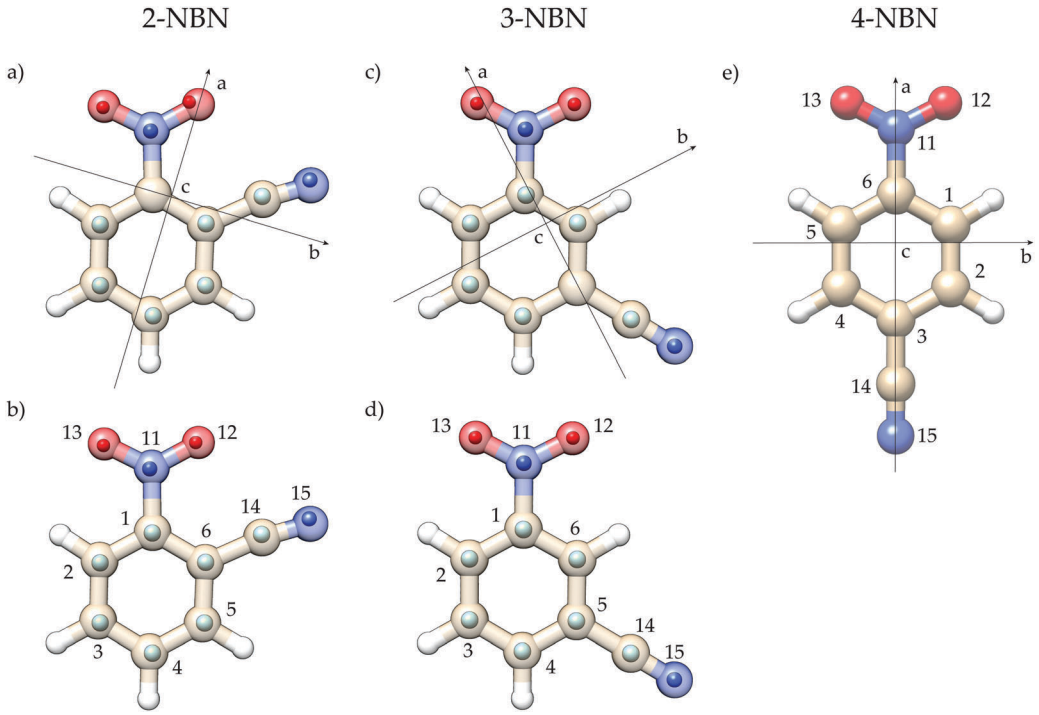

Fig. 2 Comparison of the calculated (background) and the experimentally determined (spheres, foreground) atom positions, excluding hydrogen, for 2-NBN (a) and (b), and 3-NBN (c) and (d). The calculated molecular structure of 4-NBN is also included in (e). All calculated atom positions are obtained from B3LYP/aug-cc-pVTZ geometry optimizations. Experimental atom positions determined *via* the planar Kraitchman equations (r_s-structure) are given in (a) and (c), and *via* the mass-dependent least-squares fit approach ($r_m^{(1)}$-structure) in (b) and (d). Also included is a reference to the inertial axis frames in (a), (c) and (e) and the atom labels in (b), (d) and (e).

molecule's inertial axes can impact upon the reliability of the r_s-coordinates determined.[27,28] In spite of this behaviour and the large inertial defect, the planar approach only generates an imaginary component for the C_1 atom of 2-NBN. Thus structural parameters that rely on the position of the C_1 atom could not be evaluated, whereas all the other r_s coordinates for heavy atoms could be evaluated. The r_s-structure of 2-NBN produces some unexpected behaviour, especially for the nitro group where the $r_s(N_{11}-O_{13})$ bond length is over 0.1 Å larger than the $N_{11}-O_{12}$ bond length. Although some degree of steric interaction between the nitrile and nitro group of 2-NBN might be expected, it is unlikely to be to the extent that the r_s-structure indicates. Instead of only one bond reducing in length, it is more plausible that both reduce in length in order to maintain the symmetry of the resonance structure for the nitro group. Differences in the determined r_s(N–O) bond lengths for molecules with a nitro group are not uncommon, especially for molecules similar in size to NBN where the mass of the nitro group plays a significant role in determining the orientation of the molecule's inertial axis system. When comparing the structural parameters of a nitro group between molecules, the O···O distances are often used instead of the N–O distances.[14,29,30]

For 2-NBN, a value of 1.985(4) Å is determined for the r_s(O···O) distance. Although this distance has a relatively small uncertainty value, it should be considered with care as it does not follow any logical trend when considering the O···O distances reported for other nitro containing molecules.[30] More importantly, the r_s(O···O) distance deviates significantly from the determined $r_m^{(1)}$ (2.137(9) Å) and calculated r_e (2.166 Å) O···O distances of this investigation. Cox and Waring[30] list the structural parameters reported for a series of molecules containing a nitro group (R-NO_2), and discuss how the electronegativity of the attached group (R) affects these parameters. One of the largest O···O distances reported was 2.188 Å for NO_2F,[31] where the R group (fluorine) is extremely electronegative. At the opposite end of the scale, the smallest O···O distance of 2.090 Å was reported for NO_2^- and determined *via* a neutron diffraction study.[32] The electronegativity of benzonitrile falls between these two extremes, yet the r_s(O···O) distance determined for 2-NBN is considerably smaller than the distance reported for NO_2^-.

A mass-dependent structural fit is less susceptible to the effects that reduce the accuracy of the r_s-coordinates as it takes into account the inertial defect. This approach can be employed to yield the $r_m^{(1)}$ geometry. For 2-NBN, a least-squares fit of the structure to the rotational constants and additional parameters was performed in the STRFIT program.[24] The additional parameters (c_a = 0.05(2) and c_b = 0.32(2) $\mu^{1/2}$ Å) account for the isotope-dependent rovibrational contribution to the molecule's moments of inertia.[33] From the least-squares fit method we obtain a complete set of reliable structural parameters, which can be directly compared to those determined *via* quantum-chemical calculations (refer to Tables S6 and S7 in the ESI†). The $r_m^{(1)}$-coordinates produce the expected resonance structure for the nitro group, as both the N–O bonds are essentially

equivalent within the errors, and also a more realistic O···O distance of 2.137(9) Å. Interestingly, the more reasonable $r_m^{(1)}$(O···O) value determined here is still considerably smaller than those reported for other nitrobenzene derivatives. For example, 4-nitroanisole ($NO_2C_6H_4OCH_3$) displays an $r_m^{(1)}$(O···O) distance of 2.167(3) Å,[14] which is larger than the distance determined for 2-NBN by approximately 0.03 Å. Considering that benzonitrile is a more electronegative moiety than anisole, a larger O···O might be expected for 2-NBN. However, the steric interaction of the nitro and nitrile substituents restricts the O···O distance in 2-NBN, this is made especially clear by the increase in the $r_m^{(1)}$(O···O) distance observed for 3-NBN (2.185(6) Å).

A recent gas electron diffraction study of nitroxoline reports an alternative consequence of steric interaction between a nitro group and the hydrogen atom of a neighbouring aromatic ring in the form of a non-planar dihedral angle.[34] The nitro group of nitroxoline is twisted by an angle of 8 ± 3° with respect to the plane of the aromatic ring it is bonded to. For 2-NBN, there is no such twisting of the nitro group observed, instead it is the bond lengths and angles of the respective substituents that are most affected. While the quantum-chemical calculations predict the structural parameters of the phenyl ring quite accurately, they appear limited when considering the influence of these highly electronegative, neighbouring substituents. Calculations have overestimated each of the bond lengths and distances of the nitro group (including C_1-N_{11}, $N_{11}-O_{12}$, $N_{11}-O_{13}$ and $O_{12}\cdots O_{13}$, refer to Table S6 in the ESI†) for 2-NBN.

In the case of 3-NBN these limitations are less apparent, although there are still discrepancies observed for the nitro group (see Table S8 in the ESI†). According to the experimentally determined rotational constants of 3-NBN, the magnitude of its inertial defect (−0.42 μÅ^2) is significantly smaller than that of 2-NBN. The smaller inertial defect, however, does not prevent the planar approach of Kraitchman's equations from producing an imaginary component for the C_5 atom. Thus, structural parameters that involve the C_5 atom could not be evaluated. When performing the least-squares fit method for 3-NBN the additional parameter included was c_a = 0.030(4) μ$^{1/2}$Å. Both methods used to provide experimentally determined structures for 3-NBN produce structural parameters that adhere to the expected resonance structure of the nitro group. Although the nitro groups of the experimentally determined structures are very similar, the structures of the phenyl ring differ quite significantly. The determined r_s-coordinates for the phenyl ring produce an incomplete structure with larger errors. Similar to 2-NBN, the $r_m^{(1)}$-structure of the phenyl ring is closely matched by the predicted equilibrium (r_e) structure, and it is now the nitro group alone where discrepancies arise. For a direct comparison between the experimentally determined and calculated atom positions for 2-NBN and 3-NBN refer to Fig. 2.

Comparing the structural parameters for the phenyl rings of the different NBN molecules can provide information on the electron-withdrawing strength of the respective substituents. As previously mentioned the experimental parameters of the phenyl ring for both 2- and 3-NBN are in good agreement with the calculated parameters. Thus, the parameters predicted for

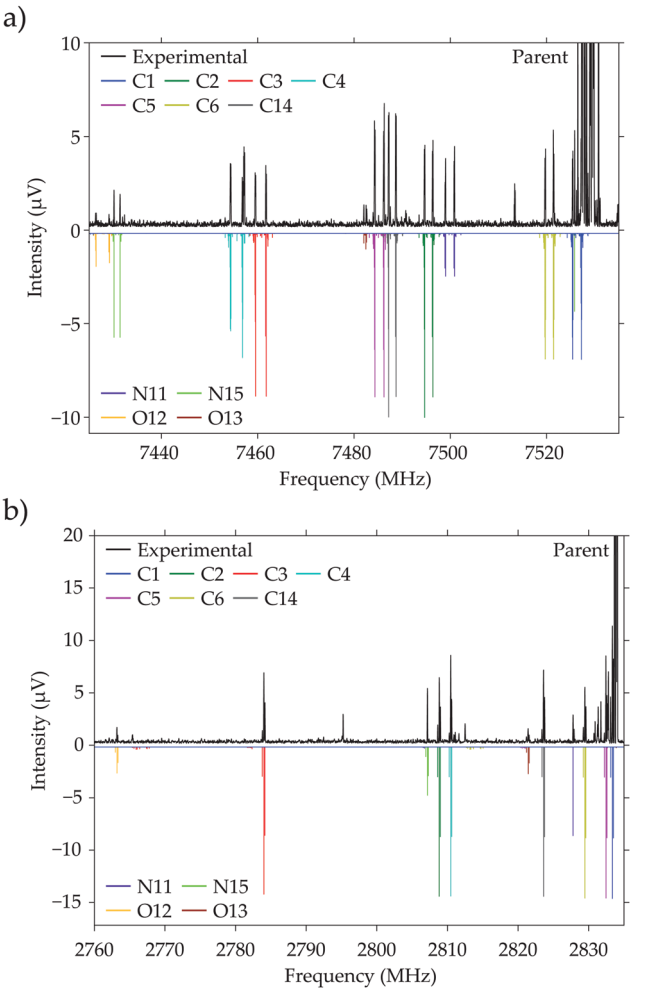

Fig. 3 Satellite lines of singly substituted ^{13}C, ^{15}N, ^{18}O isotopologues of (a) 2-NBN and (b) 3-NBN. Displayed in (a) are the $J'_{Ka',Kc'} \leftarrow J_{Ka,Kc} = 5_{15} \leftarrow 4_{14}$ and $5_{05} \leftarrow 4_{04}$ transitions, and displayed in (b) is the $J'_{Ka',Kc'} \leftarrow J_{Ka,Kc} = 1_{11} \leftarrow 0_{00}$ transition.

the phenyl ring of 4-NBN with quantum-chemical calculations can be used to validate the observation of possible trends. The carbon–carbon (C–C) bond lengths of the phenyl ring differ noticeable for each NBN molecule (refer to Tables S6, S8 and S10 in the ESI†). For each NBN molecule, the longest of the C–C bonds for the phenyl ring are consistently bonded to the nitrile group. This is a strong indicator that the nitro group is the most electron-withdrawing of the two substituents.

When comparing the structures of 2-, 3-, and 4-NBN we consider the structures obtained *via* the least-squares fitting method as well as those obtained *via* quantum-chemical calculations (Table 3). The calculated structural parameters of both substituents are almost unchanged regardless of their respective positions on the phenyl ring. However, this is contradictory to the experimental structures. The nitro group of NBN is what exhibits the most noticeable structural changes according to its position. For the nitrile group, the most revealing difference is in the ∠CCN value. Here, 2-NBN exhibits a significant deviation from 180° for the ∠CCN angle, whereas 3- and 4-NBN do not show this

Table 3 Comparison of selected structural parameters determined experimentally for 2- and 3-NBN with those determined *via* quantum-chemical calculations for 4-NBN, as well as a selection taken from an X-ray crystallography study.[15] All quantum chemical calculations utilize the B3LYP hybrid functional with the aug-cc-pVTZ basis set

	2-NBN		3-NBN		4-NBN	
Parameter[a]	$r_m^{(1)}$	B3LYP	$r_m^{(1)}$	B3LYP	X-ray[15]	B3LYP
C–NO_2	1.471(3)	1.479	1.483(4)	1.480	1.483(13)	1.480
N–O[b]	1.204(6)	1.220	1.231(6)	1.220	1.214(15)	1.220
O···O	2.137(9)	2.166	2.185(6)	2.166	—	2.167
∠ONO	125.1(5)	123.12	125.1(5)	125.14	124(1)	125.09
C–CN	1.439(4)	1.430	1.431(2)	1.431	1.438(12)	1.430
C–N	1.152(6)	1.152	1.152(3)	1.152	1.155(15)	1.152
∠CCN	171.7(5)	171.70	179.6(3)	179.57	179(1)	180.00

[a] Bond lengths in Å and angles in degrees. [b] Average of the two N–O bond lengths obtained.

deviation (see Table 3), which is attributed to the steric interaction with the neighbouring nitro group. Our experimental value for the ∠CCN angle of 3-NBN (179.6(3)°) is essentially the same as the ∠CCN angle reported for 4-NBN (179(1)°) in the X-ray crystallography study.[15] Thus, the *meta* position is already a sufficient distance away from the nitro group to prevent this steric interaction.

For the nitro group it is important to note that its structural parameters are especially sensitive to changes in its local electron density.[14,30] In general, increasing the electronegativity of the species connected to the nitro group results in changes to its structure, such as a decrease in the N–O bond length and an increase in the ONO angle and the O···O distance. The smaller $r_m^{(1)}$(N–O) bond length of 2-NBN (1.204(6) Å) compared to 3-NBN (1.231(6) Å) suggests this change to the structural arrangement of NBN could be considered as equivalent to an increase in electronegativity of the benzonitrile moiety. A smaller $r_m^{(1)}$(O···O) distance of 2-NBN (2.137(9) Å) compared to 3-NBN (2.185(6) Å) would seem to negate this. However, considering the magnitude of the decrease in $r_m^{(1)}$(N–O) bond lengths and the constant $r_m^{(1)}$(∠ONO) angle observed (125.1(5)°), it is likely that the aforementioned steric interaction prevents an increase in the O···O distance of 2-NBN. Thus, the observed changes can still be rationalised by an effective increase in electronegativity moving from the *meta*- to the *ortho*-benzonitrile configuration, which forces the nitro and nitrile substituents to compete more directly for the electron density of the phenyl ring.

5 Conclusions

The high-resolution broadband spectra of 2- and 3-NBN were recorded. For both molecules singly substituted ^{13}C, ^{15}N, and ^{18}O isotopologues in their natural abundance were observed and subsequently assigned. The accurate rotational parameters obtained for the isotopologues meant that both the substituted (r_s) and mass-dependent least-squares fit ($r_m^{(1)}$) structures could be obtained. Results from the least-squares fitting approach provided a complete set of structural parameters for both molecules, and with reduced errors the structures were also considered more reliable. The experimentally determined structures were then compared with each other and the structures obtained *via* quantum-chemical calculations. Differences in the experimentally determined NQCCs were the first indication that the local electronic environments of the nitrogen nuclei were affected by the change in the structural arrangement of NBN. After further analysis of the substituents' structural parameters, it became clear that the structure of the nitro group of NBN was sensitive to the position of the nitrile group on the phenyl ring. A degree of steric interaction between the nitrile and nitro groups was detected within 2-NBN as a ∠CCN angle significantly smaller than 180° was observed, whereas the ∠CCN angle of 3-NBN was essentially linear. In addition to this steric interaction, having the substituents bonded to adjacent carbons on the phenyl ring also appeared to increase competition for the ring's electron density. A result of this competition was observable differences in the structures of the respective nitro groups, such as smaller N–O bond lengths for 2-NBN (1.204(6) Å) compared to 3-NBN (1.231(6) Å). This behaviour has been previously observed in nitro groups that are bonded to moieties of differing electronegativities.[14,30] In the case of 2- and 3-NBN the moiety remains the same, but the proximity of the electron-withdrawing nitrile to the nitro group has altered. Thus, the consequent changes to the structure of the nitro group were then rationalised as being comparable to an increase in the electronegativity of the benzonitrile moiety when moving from the *meta* to the *ortho* configuration. Considering how common nitro group containing proteins are throughout the field of biochemistry, understanding the structural impact nearby substituents can have on a nitro group could be helpful when attempting to interpret the behaviour of an entire protein on a larger scale.

Conflicts of interest

There are no conflicts to declare.

Acknowledgements

We acknowledge the use of the GWDG computer cluster and also acknowledge Dr Cristóbal Pérez and Dr Sérgio R. Domingos for helpful discussion. Open Access funding provided by the Max Planck Society.

References

1 J. Raap, S. Nieuwenhuis, A. Creemers, S. Hexspoor, U. Kragl and J. Lugtenburg, Synthesis of isotopically labelled l-phenylalanine and l-tyrosine, *Eur. J. Org. Chem.*, 1999, 2609–2621.
2 D. Dini, F. Decker, F. Andreani, E. Salatelli and P. Hapiot, A comparative study of isomeric polydialkylterthiophenes with regular regiochemistry of substitution. Electrochemical synthesis, *Polymer*, 2000, **41**(17), 6473–6480.
3 V. Krishnakumar, G. Keresztury, T. Sundius and R. Ramasamy, Simulation of IR and Raman spectra based on scaled DFT force

fields: a case study of 2-(methylthio)benzonitrile, with emphasis on band assignment, *J. Mol. Struct.*, 2004, **702**(1), 9–21.
4 Y. Sert and F. Ucun, Vibrational spectroscopic investigation of *p*-, *m*- and *o*-nitrobenzonitrile by using Hartree–Fock and density functional theory, *Indian J. Phys.*, 2013, **87**(8), 809–818.
5 H. L. Bethlem, G. Berden and G. Meijer, Decelerating neutral dipolar molecules, *Phys. Rev. Lett.*, 1999, **83**, 1558.
6 N. Vanhaecke, U. Meier, M. Andrist, B. H. Meier and F. Merkt, Multistage Zeeman deceleration of hydrogen atoms, *Phys. Rev. A: At., Mol., Opt. Phys.*, 2007, **75**, 031402.
7 D. DeMille, D. R. Glenn and J. Petricka, Microwave traps for cold polar molecules, *Eur. Phys. J. D*, 2004, **31**, 375–384.
8 K. Enomoto and T. Momose, Microwave Stark decelerator for polar molecules, *Phys. Rev. A: At., Mol., Opt. Phys.*, 2005, **72**, 061403.
9 H. Odashima, S. Merz, K. Enomoto, M. Schnell and G. Meijer, Microwave lens for polar molecules, *Phys. Rev. Lett.*, 2010, **104**, 253001.
10 J. B. Graneek, S. Merz, D. Patterson, T. Betz and M. Schnell, Simulating spatial microwave manipulation of polyatomic asymmetric-top molecules using a multi-level approach, *ChemPhysChem*, 2016, **17**, 3624–3630.
11 C. Pérez, S. Lobsiger, N. A. Seifert, D. P. Zaleski, B. Temelso, G. C. Shields, Z. Kisiel and B. H. Pate, Broadband Fourier transform rotational spectroscopy for structure determination: the water heptamer, *J. Chem. Phys. Lett.*, 2013, **571**, 1–15.
12 S. Zinn, T. Betz, C. Medcraft and M. Schnell, Structure determination of trans-cinnamaldehyde by broadband microwave spectroscopy, *Phys. Chem. Chem. Phys.*, 2015, **17**(24), 16080–16085.
13 S. R. Domingos, C. Pérez, C. Medcraft, P. Pinacho and M. Schnell, Flexibility unleashed in acyclic monoterpenes: conformational space of citronellal revealed by broadband rotational spectroscopy, *Phys. Chem. Chem. Phys.*, 2016, **18**, 16682–16689.
14 J. B. Graneek, C. Pérez and M. Schnell, Structural determination and population transfer of 4-nitroanisole by broadband microwave spectroscopy and tailored microwave pulses, *J. Chem. Phys.*, 2017, **147**(15), 154306.
15 T. Higashi and K. Osaki, *p*-Nitrobenzonitrile, *Acta Crystallogr.*, 1977, **33**(7), 2337–2339.
16 D. Schmitz, A. Shubert, T. Betz and M. Schnell, Multi-resonance effects within a single chirp in broadband rotational spectroscopy: the rapid adiabatic passage regime for benzonitrile, *J. Mol. Spectrosc.*, 2012, **280**, 77–84.
17 G. G. Brown, B. C. Dian, K. O. Douglass, S. M. Geyer, S. T. Shipman and B. H. Pate, A broadband Fourier transform microwave spectrometer based on chirped pulse excitation, *Rev. Sci. Instrum.*, 2008, **79**(5), 053103.
18 M. J. Frisch, G. W. Trucks, H. B. Schlegel, G. E. Scuseria, M. A. Robb, J. R. Cheeseman, G. Scalmani, V. Barone, B. Mennucci, G. A. Petersson, H. Nakatsuji, M. Caricato, X. Li, H. P. Hratchian, A. F. Izmaylov, J. Bloino, G. Zheng, J. L. Sonnenberg, M. Hada, M. Ehara, K. Toyota, R. Fukuda, J. Hasegawa, M. Ishida, T. Nakajima, Y. Honda, O. Kitao, H. Nakai, T. Vreven, J. A. Montgomery, J. E. Peralta, F. Ogliaro, M. Bearpark, J. J. Heyd, E. Brothers, K. N. Kudin, V. N. Staroverov, R. Kobayashi, J. Normand, K. Raghavachari, A. Rendell, J. C. Burant, S. S. Iyengar, J. Tomasi, M. Cossi, N. Rega, J. M. Millam, M. Klene, J. E. Knox, J. B. Cross, V. Bakken, C. Adamo, J. Jaramillo, R. Gomperts, R. E. Stratmann, O. Yazyev, A. J. Austin, R. Cammi, C. Pomelli, J. W. Ochterski, R. L. Martin, K. Morokuma, V. G. Zakrzewski, G. A. Voth, P. Salvador, J. J. Dannenberg, S. Dapprich, A. D. Daniels, O. Farkas, J. B. Foresman, J. V. Ortiz, J. Cioslowski and D. J. Fox, *Gaussian 09*, Wallingford CT, 2009.
19 W. C. Bailey, DFT and HF-DFT calculations of ^{14}N quadrupole coupling constants in molecules, *Chem. Phys.*, 2000, **252**, 57–66.
20 W. C. Bailey, Calculation of nuclear quadrupole coupling constants in gaseous state molecules, http://nqcc.wcbailey.net/.
21 R. Kannengießer, W. Stahl, H. V. L. Nguyen and W. C. Bailey, ^{14}N quadrupole coupling in the microwave spectra of *n*-vinylformamide, *J. Mol. Spectrosc.*, 2015, **317**, 50–53.
22 C. M. Western, PGOPHER, a program for simulating rotational structure, http://pgopher.chm.bris.ac.uk.
23 H. M. Foley, Note on the nuclear electric quadrupole spectrum of a homonuclear diatomic molecule in a magnetic field, *Phys. Rev.*, 1947, **71**(11), 747–751.
24 Z. Kisiel, Prospe. programs for rotational spectroscopy, http://info.ifpan.edu.pl/kisiel/prospe.htm.
25 J. Kraitchman, Determination of molecular structure from microwave spectroscopic data, *Am. J. Phys.*, 1953, **21**, 17–24.
26 T. Oka, On negative inertial defect, *J. Mol. Struct.*, 1995, **352–353**(supp. C), 225–233.
27 O. Desyatnyk, L. Pszczółkowski, S. Thorwirth, T. M. Krygowski and Z. Kisiel, The rotational spectra, electric dipole moments and molecular structures of anisole and benzaldehyde, *Phys. Chem. Chem. Phys.*, 2005, **7**, 1708–1715.
28 J. Demaison and H. D. Rudolph, When is the substitution structure not reliable?, *J. Mol. Spectrosc.*, 2002, **215**(1), 78–84.
29 D. J. Millen and J. R. Morton, The microwave spectrum of nitric acid, *J. Chem. Soc.*, 1960, 1523–1528.
30 A. P. Cox and S. Waring, Microwave spectrum and structure of nitromethane, *J. Chem. Soc., Faraday Trans. 2*, 1972, **68**, 1060–1071.
31 A. C. Legon and D. J. Millen, The microwave spectrum, strucutre, and dipole moment of nitryl fluoride, *J. Chem. Soc.*, 1968, 1736–1740.
32 M. I. Kay and B. C. Frazer, A neutron diffraction study of the low temperature phase of $NaNO_2$, *Acta Cryst.*, 1961, **14**, 56–57.
33 J. K. G. Watson, A. Roytburg and W. Ulrich, Least-squares mass-dependence molecular structures, *J. Mol. Spectrosc.*, 1999, **196**(1), 102–119.
34 D. S. Tikhonov, D. I. Sharapa, A. A. Otlyotov, P. M. Solyankin, A. N. Rykov, A. P. Shkurinov, O. E. Grikina and L. S. Khaikin, Nitroxoline molecule: planar or not? A story of battle between π–π conjugation and interatomic repulsion, *J. Phys. Chem. A*, 2018, 1691–1701.